

Study of Ca doping on A- site on the structural and physical properties of BLTMNZ ceramics

P. Kumari¹, R. Rai^{1*}, A. L. Kholkin², A. Tiwari³

¹School of Physics, Shoolini University, Solan, HP, India

²Department of Glass and Ceramics, Aveiro University, Aveiro, Portugal

³Biosensors and Bioelectronics Centre, IFM, Linkopings Universitet, Linkoping 58183, Sweden

*Corresponding author. E-mail: rshyam1273@gmail.com

Received: 06 October 2013, Revised: 27 November 2013 and Accepted: 04 December 2013

ABSTRACT

The ferroelectric Ca doped ($\text{Ba}_{0.9575}\text{La}_{0.04}\text{X}_{0.0025}$) ($\text{Ti}_{0.815}\text{Mn}_{0.0025}\text{Nb}_{0.0025}\text{Zr}_{0.18}$) $_{0.99}\text{O}_3$ was prepared by a high-temperature solid state reaction technique. For the understanding of the electrical and dielectric property, the relation between the crystal structures, electrical transition and ferroelectric transitions with increasing temperature (-160 to 35°C) have been analyzed. X-ray diffraction analysis of the powders suggests the formation of a single-phase material with monoclinic structure. Capacitance and $\tan\delta$ of the specimens were measured in the temperature range from -160 to 35°C at frequencies $1\text{ kHz} - 1\text{ MHz}$. Detailed studies of dielectric and electrical properties indicate that the Curie temperature shifted to higher temperature with the increase in frequency. Moreover, the dielectric maxima dropped down rapidly initially and the dielectric peaks became extremely broad. The AC conductivity increases with increase in frequency. The low value of activation energy obtained for the ceramic samples could be attributed to the influence of electronic contribution to the conductivity. Copyright © 2014 VBRI press.

Keywords: Dielectric properties; Perovskite; lead-free ceramics; high dielectrics.



Poonam Kumari did M.Sc. (Physics and electronics) from Punjab University, Chandigarh. Presently she is pursuing M. Phil. (Physics) from School of Physics, Shoolini University, Solan since August 2012. Her current research interest is devoted on high dielectric and ferroelectric materials by using the solid state reaction method.



Radheshyam Rai had joined the National Physical Laboratory in 2003 during the Ph.D. He did his Ph.D from Magadh University Bodh Gaya in 2004 in physics. During his Ph.D he worked on PLZT ferroelectric materials with different dopants and also worked on LPG and CNG gas sensor devices in National Physical Laboratory and Indian Institute of Technology, New Delhi. He has quite significant list of publications and research activities. After that he joined as Young Scientist in Department of

Physics, Indian Institute of Technology, Delhi. During this period he worked on ferromagnetic materials for devices application. Presently he is working as Post-Doctoral Fellowship at Universidade de Aveiro, under the Fundação para a Ciência e Tecnologia, Lisboa, Portugal. During this period he is working on nonlead based piezoelectric materials for energy harvesting and ferromagnetic materials.



Ashutosh Tiwari is Associate Professor and Group Leader, Smart Materials and Biodevices at the world premier Biosensors and Bioelectronics Centre, Linköping University, Sweden; Editor-in-Chief, *Advanced Materials Letters*; Secretary General, International Association of Advanced Materials; a materials chemist and docent in the Applied Physics from Linköping University, Sweden. Dr. Tiwari is honoured as visiting professor at National Institute for Materials Science, Japan; guest Professor at

University of Jinan, China; Adjunct Professor in the DCR University of Science and Technology, India; and Director, Vinoba Bhawe Research Institute, India. Just after completed his doctorate degree, he joined as young scientist at National Physical Laboratory, India and later moved to University of Wisconsin, USA for postdoctoral research. He is actively engaged as reviewer, editor and member of scientific bodies around the world. Prof. Tiwari obtained various prestigious fellowships including JSPS (regular and bridge fellow), Japan; SSF & SI, Sweden; and Marie Curie, The European Commission. In his academic carrier, he has published over 350 articles including journal articles, patents, book chapters and conference proceedings in the field of materials science and technology. He edited/authored more than twenty books on the advanced state-of-the-art of materials science with several publishers. He became the book series editor of *Advanced Materials Series*, working group member of the technology integration of TD1003, European Cooperation in Science and Technology and a founder member of Advanced Materials World Congress, Indian Materials Congress, International Conference on Smart Materials and Surfaces famous international events of materials science and engineering. Dr. Tiwari is receipt of high-status 'The Nano Award', 'Innovation in Materials Science Award' and 'Advanced Materials Medal'.

Introduction

Systematic and extensive studies have been carried out on lead based ABO_3 ceramics, composites, single crystals, thin films. These compounds are toxic, hazardous and non-recyclable, as they contain lead. To control the use of lead contained ABO_3 ceramics, lead-free ceramics are being investigated. Barium zirconate titanate (BZT) is one such interesting ferroelectric material due to its high dielectric constant [1], which make it's a very attractive material for use in capacitor applications such as boundary layer capacitors and multilayer ceramic capacitors. Due to the environmental concern, this material is also beneficial compare to lead based materials [2, 3]. BaTiO_3 ceramics were famous material before the discovery of PZT [4-6]. BZT is an attractive ceramic due to large change in structural and physical properties after doping on A or B-site. When the Zr content is less than 10 mol%, the BZT ceramics show normal ferroelectric behavior and dielectric anomalies corresponding to cubic to tetragonal, tetragonal to orthorhombic, and orthorhombic to rhombohedral phase transitions. At around 27 mol%, Zr-doped BZT ceramics exhibit typical diffuse paraelectric to ferroelectric phase transition behavior, whereas Zr-rich compositions exhibit typical relaxor-like behavior in which T_c shifts to higher temperature with increase of frequency [7-9]. The electrical properties of these type of ceramics are very sensitive to both microstructure and defect chemistry of the materials, which are strongly influenced by processing parameters, such as chemical composition and sintering conditions. Temperature dependent dielectric study showed normal ferroelectric to paraelectric transition well above the room temperature except for barium bismuth tantalate (BBT) [10, 11].

Spontaneously polarized state is realized in ferroelectrics as a domain structure [12]. It is extensively used in high dielectric constant capacitors, multilayer ceramic capacitors (MLCC) and energy storage devices. BaTiO_3 having the perovskite structure with tetragonal symmetry at room temperature, possesses a relatively high dielectric constant [13]. By the different doping in BZT ceramics, we can improve the material performance or dielectric properties [9,14,15]. BZT based tunable ferroelectric materials with moderate dielectric constant and low dielectric loss have been obtained by manipulating the doping amount of suitable rare-earth ions up to 4% [16]. Recently many researchers studied the effect of rare-earth doping on $(\text{Ba}_{1-x}\text{Ln}_x)\text{Zr}_{0.2}\text{Ti}_{0.8-x/4}\text{O}_3$ ($\text{Ln} = \text{La}, \text{Sm}, \text{Eu}, \text{Dy}, \text{Y}$) ceramics. Chou et al. reported the diffuseness of the phase transition and the degree of ferroelectric relaxor behavior are enhanced by the doping [16].

The main purpose of this research is synthesis and characterization of A-site doped CaO doped $(\text{Ba}_{0.9575}\text{La}_{0.04}\text{Ca}_{0.0025})(\text{Ti}_{0.815}\text{Mn}_{0.0025}\text{Nb}_{0.0025}\text{Zr}_{0.18})_{0.99}\text{O}_3$, (BLCTMNZ) ceramics as a kind of suitable tunable dielectric materials for tunable ceramic capacitors. Samples were obtained from solid state reaction methods. Structural analysis and dielectric characterization of the proposed solid solution have been performed for compounds obtained by solid-state reaction.

Experimental

The barium zirconate titanate ceramics were prepared by solid state reaction method. Suitable stoichiometric amounts of high purity oxides of TiO_2 (Aldrich 99.9 %), BaCO_3 (Aldrich 99.9 %), CaCO_3 (Aldrich 99.9 %), ZrO_2 (Aldrich 99.9 %), Nb_2O_5 (Aldrich 99.9 %), Mn_2O_3 (Aldrich 99.9 %), and La_2O_3 (Aldrich 99.9 %) raw materials were used as starting materials according to the formula $(\text{Ba}_{0.9575}\text{La}_{0.04}\text{Ca}_{0.0025})(\text{Ti}_{0.815}\text{Mn}_{0.0025}\text{Nb}_{0.0025}\text{Zr}_{0.18})_{0.99}\text{O}_3$. Weighted source powders were mixed by ball milling for ~24 hrs using ZrO_2 balls in acetone media. The mixed powders were dried and calcined for 6 hrs at ~1100 °C. The calcined powder was grounded in a mortar pestle to obtain fine powder. The grinding process was repeated for ~8 hrs in presence of PVA as binding liquid. After grinding the powders were uniaxially pressed into pellets of approximately 10mm diameter and sintered at a temperature of 1200°C for 2 hrs in a high temperature muffle furnace. The sintered pellets were used to characterize the structural and microstructural properties of the compound. The X-ray diffraction pattern of the compounds were recorded at room temperature using X-ray powder diffractometer with $\text{CuK}\alpha$ ($\lambda = 1.5418\text{\AA}$) radiation (Rigaku Miniflex, Japan) in a wide range of Bragg angles 2θ ($20^\circ \leq 2\theta \leq 60^\circ$) at a scanning rate of 2°min^{-1} . Silver painted electrodes were applied to the both faces of sintered samples. The dielectric properties were studied in the frequency range 1kHz-1MHz and in the temperature range -160 to 35 °C using an impedance analyzer PSM1735.

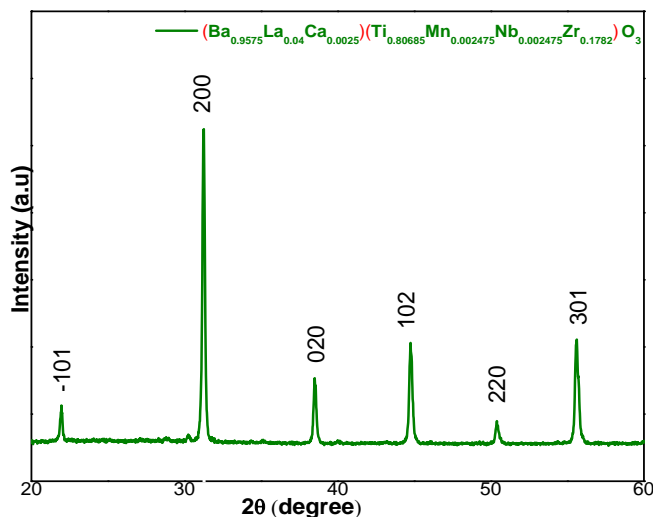


Fig. 1. XRD patterns of sintered Ca doped $(\text{Ba}_{0.9575}\text{La}_{0.04}\text{Ca}_{0.0025})(\text{Ti}_{0.815}\text{Mn}_{0.0025}\text{Nb}_{0.0025}\text{Zr}_{0.18})\text{O}_3$ ceramics.

Results and discussion

Fig. 1 shows the room temperature XRD patterns of the Ca doped $(\text{Ba}_{0.9575}\text{La}_{0.04})(\text{Ti}_{0.815}\text{Mn}_{0.0025}\text{Nb}_{0.0025}\text{Zr}_{0.18})\text{O}_3$ perovskite type ceramics. All the reflection peaks were indexed using observed inter-planar spacing d and lattice parameters of Ca doped BLTMNZ were determined using a least squares refinement method by using a computer program package Powder¹⁷. Finally, monoclinic unit cell

was selected on the basis of good agreement between observed (obs) and calculated (cal) interplanar spacing d (i.e., $\Sigma\Delta d = \Sigma (d_{\text{obs}} - d_{\text{cal}}) = \text{minimum}$) of the peaks. The refined lattice parameters of Ca doped $(\text{Ba}_{0.9575}\text{La}_{0.04})(\text{Ti}_{0.815}\text{Mn}_{0.0025}\text{Nb}_{0.0025}\text{Zr}_{0.18})\text{O}_3$ are given in **Table 1**.

Table 1. Comparison of some observed and calculated d -values (in Å) of some reflections of sintered Ca doped $(\text{Ba}_{0.9575}\text{La}_{0.04})(\text{Ti}_{0.815}\text{Mn}_{0.0025}\text{Nb}_{0.0025}\text{Zr}_{0.18})\text{O}_3$ ceramics at room temperature.

Sample Name	a	b	c	d_{obs}	d_{cal}	hkl
				4.0440	4.0440	<101>
				2.8589	2.8589	<200>
$(\text{Ba}_{0.9575}\text{La}_{0.04}\text{Ca}_{0.0025})(\text{Ti}_{0.815}\text{Mn}_{0.0025}\text{Nb}_{0.0025}\text{Zr}_{0.18})\text{O}_3$	5.8403Å	4.6726Å	4.7722Å	2.3363	2.3363	<020>
				2.0230	2.0230	<102>
				1.8090	1.8091	<220>
				1.6510	1.6510	<301>

The (200) reflection line in XRD pattern were used for obtaining the average particle size by using the Debye-Scherrer equation [17],

$$t = \frac{0.9\lambda}{B \cos \theta_B} \quad (1)$$

$$B = (B_M^2 - B_S^2)^{1/2} \quad (2)$$

where t is the diameter of the particle, λ is the x-ray wavelength (0.154 nm), B_M and B_S are the measured peak broadening and instrumental broadening in radian, respectively, and θ_B is the Bragg angle of the reflection. The calculated average particle size from **Eq. (1)** is 40-42nm.

Fig. 1 illustrates the x-ray diffraction pattern of the ZnO nanostructure synthesized by chemical route. This XRD pattern shows that, all the diffraction peaks in the pattern can be assigned to hexagonal 'wurtzite' ZnO with lattice constants $a = 0.3249$ nm and $c = 0.5206$ nm, which are in good agreement with the literature values (JCPDS card No. 36-1451). In above XRD pattern, extra peak appear at $2\theta = 44^\circ$. This peak was identified as surface hydroxyl groups, which can be related to the formation of water on the ZnO nanostructure surface [18]. The presence of sharp single peaks of varying intensity in the XRD pattern indicates formation of single phase with little secondary phase. From XRD it is clear that sample have perovskite major phase.

Fig. 2 shows the variation of dielectric permittivity and dielectric loss of the samples with frequency at different temperature. It may be noted that in sample, there is a decrease in the dielectric constant with increasing frequency and temperature, which is a typical characteristic of normal dielectric. For higher frequencies i.e., 1000Hz the value of dielectric constant increases attaining maxima at -79.8°C as given in **Table 2**.

A relatively high dielectric constant at low frequencies is a characteristic of all dielectric materials. This is due to the fact that dipoles can no longer follow the field at high

frequencies [19]. The values of the dielectric constant and $\tan\delta$ were found to be strongly frequency- dependent. As can be seen in the **Fig. 2**, the values of dielectric constant decrease as the frequency is increased. The orientational polarization plays a significant role in the relaxation process. The decrease of the dielectric constant with frequency is due to a decrease of total polarization arising from dipoles and trapped charge carriers. Since, in most materials [20] the trapped charge carriers contribute to the total polarization, the polymer system normally contains a large numbers of trapping sites, therefore one may expect a large effect of the trapped charge carrier at the lowest frequency giving large values of dielectric constant [21]. However, as the frequency of the applied field increases, the dipoles will hardly be able to orient themselves in the direction of the applied field, and hence the value of the dielectric constant decreases at high frequency [22]. The value of dielectric loss is lower for higher temperature and increasing with frequency for lower value of temperature.

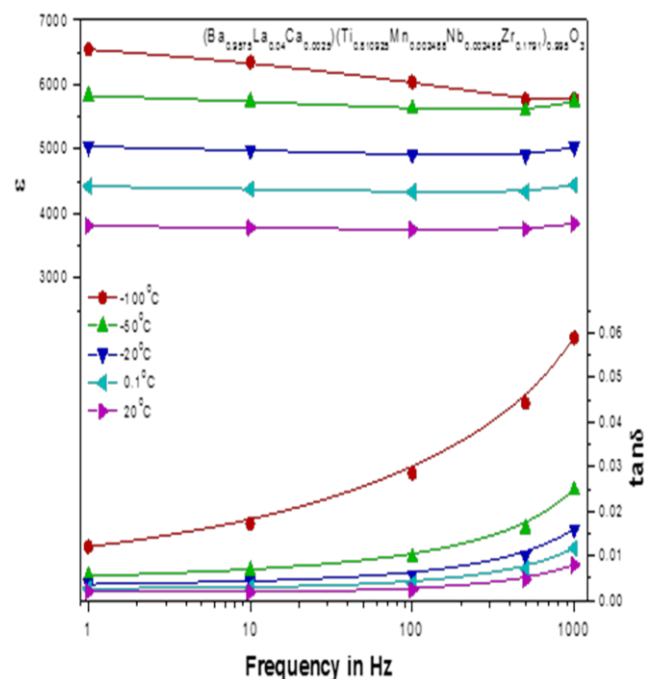


Fig. 2. Variation of dielectric permittivity (ϵ) and loss tangent $\tan(\delta)$ of Ca doped $(\text{Ba}_{0.9575}\text{La}_{0.04}\text{Ca}_{0.0025})(\text{Ti}_{0.815}\text{Mn}_{0.0025}\text{Nb}_{0.0025}\text{Zr}_{0.18})\text{O}_3$ ceramics as a function of frequency at different temperature.

Table 2. Comparison of some physical properties of Ca doped $(\text{Ba}_{0.9575}\text{La}_{0.04}\text{Ca}_{0.0025})(\text{Ti}_{0.815}\text{Mn}_{0.0025}\text{Nb}_{0.0025}\text{Zr}_{0.18})\text{O}_3$ ceramics.

Frequency(kHz)	$T_{\text{(max)}}$	$\epsilon_{\text{(max)}}$	E_a	$\tan\delta_{\text{(max)}}$	γ
1	-104.8	6557.61108	0.67	0.01348	1.40
10	-94.9	6346.11145	0.68	0.01509	1.46
100	-89.8	6094.50769	0.63	0.02169	1.50
500	-84.9	5940.10752	0.47	0.03159	1.70
1000	-79.8	6049.98645	0.35	0.04102	1.66

The temperature dependence of dielectric constant (ϵ) and loss tangent ($\tan\delta$) for the BLCTMNZ samples at constant frequencies i.e. 40Hz, 1 kHz, 10 kHz, 100 kHz, 500 kHz and 1 MHz are shown in **Fig. 3**.

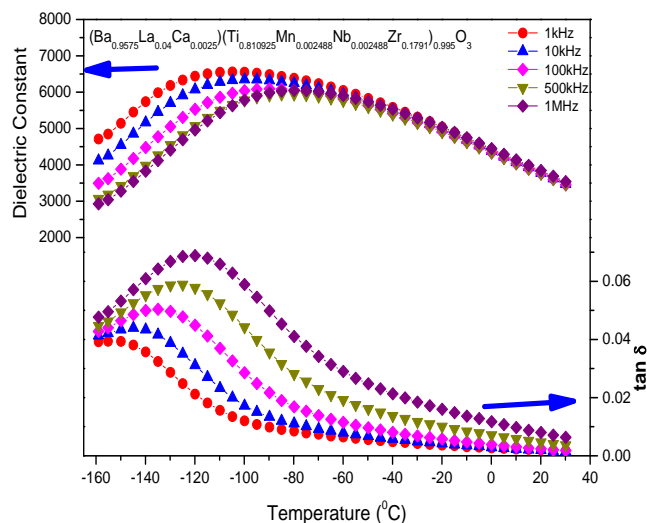


Fig. 3. Variation of dielectric permittivity (ϵ) and loss tangent $\tan(\delta)$ of Ca doped $(\text{Ba}_{0.9575}\text{La}_{0.04}\text{Ca}_{0.0025})(\text{Ti}_{0.815}\text{Mn}_{0.0025}\text{Nb}_{0.0025}\text{Zr}_{0.18})\text{O}_3$ ceramics as a function of temperature at different frequencies.

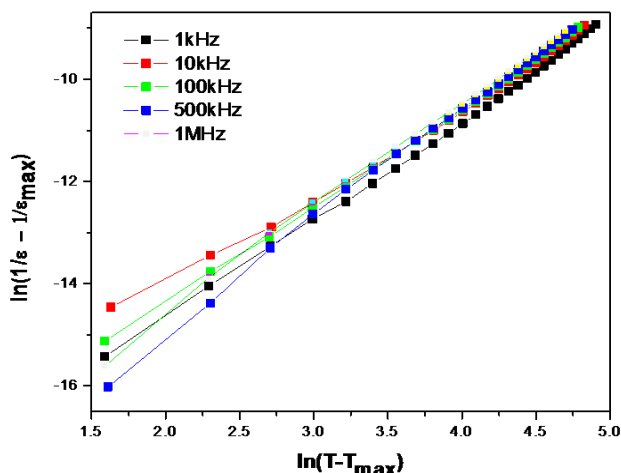


Fig. 4. Variation of $(1/\epsilon - 1/\epsilon_{\max})$ of Ca doped $(\text{Ba}_{0.9575}\text{La}_{0.04})(\text{Ti}_{0.815}\text{Mn}_{0.0025}\text{Nb}_{0.0025}\text{Zr}_{0.18})\text{O}_3$ ceramics as a function of temperature ($T - T_{\max}$) at different frequencies.

It is found that with increasing temperature, dielectric constant increases and after T_c dielectric constant decreases with increasing temperature. The dielectric constant of the system decreases with the increasing the frequency in the investigated range of (40 Hz – 1 MHz). A small shift of dielectric constant towards higher values of the (T_m) temperature (-160-35) °C corresponding to the maximum value of the permittivity ϵ_{\max} is visible with increasing the frequency. A relaxation of the dielectric constant in the ferroelectric place gives the idea that the present sample is close to the relaxor state. From the variation of $\tan \delta$ with temperature at different frequency, we observed that the values of the tangent loss ($\tan \delta$) increases with increasing frequency, indicating a normal behavior of dielectrics/ferroelectrics. But with increase of temperature,

the nature of variation shows the existence of $\tan \delta$ peak at a higher frequency. As frequencies increases the loss value also increases but after T_m $\tan \delta$ becomes closer in all frequency. The same type of relaxation of the loss also indicates that the present sample is close to the relaxor state.

The degree of disorder of the sample was evaluated using the expression $(1/\epsilon - 1/\epsilon_{\max}) (T - T_{\max})^\gamma$, where γ is a measure of diffuseness of the ferroelectric to paraelectric phase transition. The logarithmic plots related to this equation are shown in **Fig. 4**. The values of γ are found to lie between 1.4 and 1.7, which confirm the diffuse phase transition in BLCTMNZ compound as shown in **Table 2**. The maximum value of γ at frequency 500 kHz. An alternative approach was also adopted to estimate the degree of diffuseness using the relation $\ln(\epsilon - 1/\epsilon_{\max}) = (T - T_{\max})/2\delta_g^2$ in which δ_g is the Gaussian [23]. From the value of δ_g , which is related to the broadening of $\epsilon(T)$ curve, we can determine the degree of compositional fluctuations in the material.

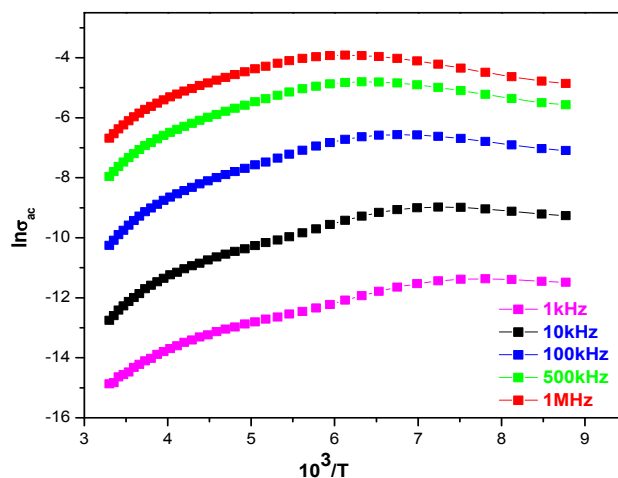


Fig. 5. Variation of ac conductivity $\ln\sigma_{ac}$ as a function of inverse of absolute temperature $10^3/T$ of Ca doped $(\text{Ba}_{0.9575}\text{La}_{0.04})(\text{Ti}_{0.815}\text{Mn}_{0.0025}\text{Nb}_{0.0025}\text{Zr}_{0.18})\text{O}_3$ ceramics at different frequencies.

The ac conductivity (σ_{ac}) of the samples was calculated from the dielectric data using the relation $\sigma_{ac} = \omega\epsilon_0\tan\delta$. **Fig. 5** shows the variation of σ_{ac} with frequency (in the frequency range 1 kHz to 1 MHz) at room temperature. It was noticed that σ_{ac} increases with increasing frequency. Also, the DC conductivity is generally increased with increasing frequency and there is a particularly small increase in σ_{ac} after about 500 kHz, where ϵ_0 is the vacuum dielectric permittivity and ω is the angular frequency. Further the activation energy (E_a) was evaluated from the $\ln\sigma_{ac}$ vs $10^3/T$ curve using the relation $\sigma = \sigma_0 e^{E_a/k_B T}$ (where k_B is the Boltzmann constant) **Fig. 5**. The values of E_a for all composition at different frequency are given in **Table 2**. The value of activation energy in the paraelectric phase is found to be very low. A low value of the activation energy has been observed in many such type of ferroelectric complex compounds. This may be due to ionic solids having a limited number of mobile ions being trapped in relatively stable potential wells during their motion through the solid. Due to a rise in

temperature the donor cations are taking a major part in the conduction process. The donors have created a level (i.e. band-donor level), which is much nearer to the conduction band. Therefore, only a small amount of energy is required to activate the donors. In addition to this, a slight change in stoichiometry in multi-metal complex oxides causes the creation of large number of donors or acceptors, which creates donor or acceptors like states in the vicinity of conduction or valance bands. These donors or acceptors may also be activated with small energy [11].

Conclusion

In this paper we discussed the structure and dielectric properties of calcium doped barium zirconate titanate ceramics.

($\text{Ba}_{0.9575}\text{La}_{0.04}\text{X}_{0.0025}$) ($\text{Ti}_{0.815}\text{Mn}_{0.0025}\text{Nb}_{0.0025}\text{Zr}_{0.18}$) $_{0.99}\text{O}_3$ (BLCTMNZ) with perovskites structure were synthesized by solid state reaction method. The crystal structure of this material is monoclinic. The dielectric permittivity $s(\epsilon)$ and loss tangent ($\tan\delta$) of BLCTMNZ ceramics as a function of temperature (-160 to -40°C) at frequencies (1 kHz – 1MHz) suggest that the compounds exhibit a phase transition of diffuse type. In this case, a typical relaxor behavior was observed. The maximum relative permittivity of these materials was high i.e. (5000 - 6000 at 40 kHz). On increasing the temperature the dielectric loss is decrease to lower value. The ac conductivity was increases with the higher value of frequency (1MHz.).

Reference

- Jarupoom, P.; Eitssayeam, S.; Pengpat, K.; Tunkasiri, T.; Cann, D.; Rujijanagul, G. *Nanoscale Res. Lett.* **2012**, 7, 59.
DOI: [10.1186/1556-276X-7-59](https://doi.org/10.1186/1556-276X-7-59).
- Yang, G.Y.; Dickey, E.C.; Randall, C.A.; Barber, D.E.; Pinceloup, P.; Henderson, M.A.; Hill, R.A.; Beeson, J.J.; Skamser, D.J. *J. App. Phys.* **2004**, 96, 7492-7499.
DOI: [10.1063/1.1809267](https://doi.org/10.1063/1.1809267).
- Yu, Z.; Guo, R.; Bhalla, A.S. *J. App. Phys.* **2000**, 88, 410-415.
DOI: [10.1063/1.1308276](https://doi.org/10.1063/1.1308276).
- Behera, A.K.; Mohanty, N.K.; Behera, B.; Nayak, P. *Adv. Mat. Lett.* **2013**, 4, 141-145.
DOI: [10.5185/amlett.2012.6359](https://doi.org/10.5185/amlett.2012.6359).
- Chamola, A.; Singh, H.; Naithani, U. *Adv. Mat. Lett.* **2011**, 2, 148-152.
DOI: [10.5185/amlett.2010.11183](https://doi.org/10.5185/amlett.2010.11183).
- Singh, N.K.; Kumar, P.; Rai, R.; Kholkin A.L. *Adv. Mat. Lett.* **2012**, 3, 315-320.
DOI: [10.5185/amlett.2012.5345](https://doi.org/10.5185/amlett.2012.5345).
- Nanakorn, N.; Jalupoom, P.; Vaneeorn, N.; Thanaboonsombut, A. *Ceramics International*. **2008**, 34, 779-782.
DOI: [10.1016/j.ceramint.2007.09.024](https://doi.org/10.1016/j.ceramint.2007.09.024).
- Badapanda, T.; Rout, S.K.; Cavalcante, L.S.; Sczancoski, J.C.; Panigrahi, S.; Sinha, T.P.; Longo, E. *Materials Chemistry and Physics*. **2010**, 121, 147-153.
DOI: [10.1016/j.matchemphys.2010.01.008](https://doi.org/10.1016/j.matchemphys.2010.01.008).
- Dobal, P.S.; Dixit, A.; Katiyar, R.S.; Yu, Z.; Guo, R.; Bhalla, A.S. *J. App. Phys.* **2001**, 89, 8085-8091.
DOI: [10.1063/1.1369399](https://doi.org/10.1063/1.1369399).
- Rout, S.K.; Sinha, E.; Hussain, A.; Lee, J.S.; Ahn, C.W.; Kim, I.W.; Woo, S. I. *J. App. Phys.* **2009**, 105, 024105-6.
DOI: [10.1063/1.3068344](https://doi.org/10.1063/1.3068344).
- Shu, L.; Wei, X.; Jin, L.; Li, Y.; Wang, H.; Yao, X. *App. Phys. Lett.* **2013**, 102, 152904-4.
DOI: [10.1063/1.4802450](https://doi.org/10.1063/1.4802450).
- Sidorkin, A. S. *Journal of Advanced Dielectrics*. **2012**, 02, 1230013.
DOI: [10.1142/s2010135x12300137](https://doi.org/10.1142/s2010135x12300137).
- Duran, P.; Capel, F.; Gutierrez, D.; Tartaj, J.; Banares, M.A.; Moure, C. *J. Mat. Chem.* **2001**, 11, 1828-1836.
DOI: [10.1039/b010172j](https://doi.org/10.1039/b010172j).
- Tsur, Y.; Dunbar, T.; Randall, C. *Journal of Electroceramics*. **2001**, 7, 25-34.
DOI: [10.1023/a:1012218826733](https://doi.org/10.1023/a:1012218826733).
- Abdelmoula, N.; Khemakhem, H.; Simon, A.; Maglione, M. *Journal of Solid State Chemistry*. **2006**, 179, 4011-4019.
DOI: <http://dx.doi.org/10.1016/j.jssc.2006.09.006>.
- Chou, X.; Zhai, J.; Jiang, H.; Yao, X. *J. App. Phys.* **2007**, 102, 084106-6.
DOI: [10.1063/1.2799081](https://doi.org/10.1063/1.2799081).
- Patterson, A.L. *Physical Review*. **1939**, 56, 978-982.
DOI: [10.1103/PhysRev.56.978](https://doi.org/10.1103/PhysRev.56.978).
- Wu, E. *POWD*, **1989**, 22, 506-510.
DOI: [10.1107/S0021889889005066](https://doi.org/10.1107/S0021889889005066).
- Amar Nath, K.; Prasad, K.; Chandra, K.P.; Kulkarni, A.R. *Bull. Mater. Sci.* **2013**, 36, 591-599.
DOI: [10.1007/s12034-013-0503-y](https://doi.org/10.1007/s12034-013-0503-y).
- Tunç, T.; Gökçen, M.; Uslu, İ. *Appl. Phys. A*. **2012**, 109, 649-653.
DOI: [10.1007/s00339-012-7087-z](https://doi.org/10.1007/s00339-012-7087-z).
- Shockley, W.; Read, W.T. *Physical Review*. **1952**, 87, 835-842.
DOI: [10.1103/PhysRev.87.835](https://doi.org/10.1103/PhysRev.87.835).
- Bhajantri, R.F.; Ravindrachary, V.; Harisha, A.; Ranganathaiah, C.; Kumaraswamy, G.N. *Appl. Phys. A*. **2007**, 87, 797-805.
DOI: [10.1142/S2010135X1241010X](https://doi.org/10.1142/S2010135X1241010X).
- YE, Z.-G.; Bokov, A.A. *Journal of Advanced Dielectrics*. **2012**, 02, 1241010.
DOI: [10.1142/S2010135X1241010X](https://doi.org/10.1142/S2010135X1241010X).

Advanced Materials Letters

Publish your article in this journal

ADVANCED MATERIALS Letters is an international journal published quarterly. The journal is intended to provide top-quality peer-reviewed research papers in the fascinating field of materials science particularly in the area of structure, synthesis and processing, characterization, advanced-state properties, and applications of materials. All articles are indexed on various databases including DOAJ and are available for download for free. The manuscript management system is completely electronic and has fast and fair peer-review process. The journal includes review articles, research articles, notes, letter to editor and short communications.

